

## Airborne Hot-Film Measurements of the Small-Scale Structure of Atmospheric Turbulence During GATE

FRANCIS J. MERCERET

*National Hurricane and Experimental Meteorology Laboratory, NOAA, Coral Gables, Fla. 33124*

(Manuscript received 9 October 1975, in revised form 27 April 1976)

### ABSTRACT

Fluctuations of temperature, horizontal velocity and vertical velocity were measured at scales from 50 m to 5 cm with airborne hot-film anemometers at altitudes of 150 and 900 m in clear air, and in subcloud air with and without rainfall. Although nearly inertial subrange spectral behavior was often present at scales smaller than 20 m, significant regions existed where inertial behavior did not appear until scales smaller than a few meters were reached. The energy dissipation rate varied intermittently by two orders of magnitude or more over scales ranging from 100 m to several kilometers. High Reynolds number intermittency effects were observed in the temperature spectra. In an anomalous region, here called a "dry hole," the microstructure of the velocity and temperature fields was radically different from that of the surrounding environment. Spectral intensity decreased by an order of magnitude and spectral shape was definitely non-inertial. Despite these changes, the probability distribution of the energy dissipation seemed to remain close to log-normal as did the distribution in the surroundings.

### 1. Introduction

This paper presents observations of the structure of atmospheric turbulence at scales smaller than 50 m during GATE. The data show regions of substantial departure from the expected inertial subrange spectral behavior. Time series of  $U'$  and the logarithm of dissipation ( $\epsilon$ ) are given along with probability distributions of  $\ln \epsilon$  and spectra of  $U'$ ,  $W'$  and  $T'$ . It is hoped that the observations may stimulate thought about the finestructure of atmospheric turbulence and eventually lead to further experimental and theoretical investigations of the phenomena observed here.

### 2. Data sources and processing

The hot-film instrumentation aboard NOAA's DC-6 during GATE has been described by Merceret (1976). On 29 July (Julian Day 210) 1974 2 h of good quality data were obtained between 1330 and 1710 GMT. The data, four 25 min segments, were obtained in the environments shown in Table 1. Spectra of the vertical velocity fluctuations ( $W'$ ), the horizontal velocity fluctuations along the aircraft heading ( $U'$ ) and the temperature fluctuations ( $T'$ ) were generated using a Spectral Dynamics SD330A<sup>1</sup> real-time analyzer. These spectra were recorded on strip charts and replotted by discarding peaks at 60 and 400 Hz and their harmonics to produce the spectra shown in this paper.

<sup>1</sup> Mention of a proprietary product does not constitute an endorsement thereof by the author or by the National Hurricane and Experimental Meteorology Laboratory.

The frequency response of the hot-film sensors is the same for all measurements reported here and is nearly flat over the frequency of interest (2 to 2500 Hz). Thus, spectra were not corrected for frequency response. The aircraft maintained a true airspeed of 92 m s<sup>-1</sup> for all measurements at 150 m and 96 m s<sup>-1</sup> ± 2 at 960 m. Radar altitude was maintained within ± 3 m, and pitch, roll and yaw did not exceed ± 3° except during turns. The data during turns were discarded. The total error from all causes except sampling is estimated to be ± 2 dB for the absolute reference of any spectrum and ± 0.5 dB within each spectrum. The sampling error depends upon the record length and ranges from a maximum of ± 7% to a minimum of ± 4% for the samples reported here which have record lengths from 33 to 133 s and an equivalent filter bandwidth of 6 Hz (Bendat and Piersol, 1966, p. 208). The cumulative error is large enough to preclude a careful check of the  $\frac{2}{3}$  spectrum ratio of  $W'$  to  $U'$ , but is quite acceptable when spectral slope analysis is used, as here, for examining deviations from inertial subrange behavior and for high Reynolds number effects.

The dissipation rate was continuously estimated from an exponential running mean of the  $W'$  spectrum at 470 Hz with a time constant of 2 s. With this short record length the error may be as large as 30% (Bendat and Piersol, 1966, p. 208) in the spectral estimate and thus nearly 50% in the estimate of  $\epsilon$  because of the power law relation [Eq. (1)] between them. The dissipation estimates assume the one-dimensional velocity

TABLE 1. Data base.

Reel no.	Time (GMT)	Altitude (m)	Environment	Precipitation	Notes
14	1340-1405	150	Clear and subcloud	no	All 150 m runs at $\sim 9^\circ\text{N}$ , $23^\circ\text{W}$
15	1449-1513	150	Clear and subcloud	yes	Includes dry hole penetration
16	1530-1554	150	Subcloud	yes	
17	1644-1708	960	Clear and above cloud	no	$\sim 10^\circ\text{N}$ , $21^\circ\text{W}$

spectra  $\phi(k)$  have the form

$$\phi(k) = \alpha_1 \epsilon^{2/3} k^{-5/3} \quad (1)$$

for wavenumbers  $k$  in the inertial subrange. Eq. (1) is converted to frequency space on the assumption that  $\alpha_1 = 0.5$  for  $U'$ , based on the results of Boston and Burling (1972). The result used here (accurate to 5%) is

$$\phi_u(f) = 6.1 \epsilon^{2/3} f^{-5/3}, \quad (2)$$

$$\phi_w(f) = \frac{1}{3} \phi_u(f) = 8.1 \epsilon^{2/3} f^{-5/3}, \quad (2a)$$

where  $\phi$  is  $\text{m}^2 \text{s}^{-2} \text{Hz}^{-1}$ ,  $f$  is  $\text{Hz}$  and  $\epsilon$  is  $\text{m}^2 \text{s}^{-3}$ , assuming  $\bar{U} = 94 \pm 4 \text{ m s}^{-1}$ . If we choose  $f = 470 \text{ Hz}$  for either  $U$  or  $W$ , we may calibrate  $\phi(470)$  in terms of dissipation. The frequency was selected high enough to be certain of being in the inertial subrange in all cases as well as having a characteristic response time not greater than the smaller averaging time used. The response time is given by Lumley and Panofsky (1964, p. 86) as  $[k^3 E(k)]^{-1/2}$ , which amounts to about 2 s for wavelengths of 21 cm (corresponding to 470 Hz at  $100 \text{ m s}^{-1}$ ) and a dissipation rate of  $1.0 \text{ cm}^2 \text{ s}^{-3}$ . This ensures that the energy at that scale is reasonably, even if not exactly, representative of the dissipation rate. The frequency of 470 Hz is also well away from powerline harmonics which might otherwise contaminate the signal. Even tape 17, which was the worst case because of its low-turbulence level, contained adequate signal at this frequency. By connecting the spectrum analyzer's log dissipation output (log of PSD at 470 Hz) to a Honeywell SAI 43 correlator in the probability distribution mode, we obtained the distribution of  $\log \epsilon$ .

Tapes 14, 15 and 16 were recorded at 150 m, an altitude that kept the aircraft below cloud base. Cloud base was estimated from nose camera film to be at  $\sim 200 \text{ m}$  as we passed under lines of precipitating and non-precipitating cumulus. The 1500 GMT SMS-1 picture shows the region near  $9^\circ\text{N}$ ,  $23^\circ\text{W}$  to be almost entirely overcast, except for sporadic openings in the clouds, while the aircraft cameras show that much of this is middle and high cloud, with the cumulus and precipitation in showers and in lines of showers. Except for brief segments (such as one in which a "dry hole" was penetrated, see below), the air and dew point temperatures were steady;  $T_a$  was  $23 \pm 1.5^\circ\text{C}$  and  $T_d$  was  $21 \pm 1.0^\circ\text{C}$ . Soundings from the *Quadra* ( $9^\circ 15'\text{N}$ ,  $22^\circ 12'\text{W}$ ) and Prof. Vize ( $8^\circ 30'\text{N}$ ,  $23^\circ 37'\text{W}$ )

at 1200 and 1800 GMT show a lapse rate of  $5-6^\circ\text{C km}^{-1}$  and a nearly uniform dew point depression of  $2-3^\circ\text{C}$  in the lowest thousand meters. There is a region at 4-6 km which is near saturation with a dry region ( $T_a - T_d \geq 9^\circ\text{C}$ ) extending upward from 6 km. Tape 17 was recorded above small scattered cumulus, most of which did not reach flight level at 960 m. The air temperature was  $19.6 \pm 1^\circ\text{C}$  and the dew point  $17.2 \pm 1^\circ\text{C}$ . The cloud field and turbulence level are consistent with the hypothesis of stability at flight level, but no soundings were available in the area where this tape was made. Without a sounding, it is difficult to draw firm conclusions about the physical environment.

During one of the low-level runs (tape 15) we penetrated a small region of warm, dry air which had unusual properties. The presence of relatively dry and probably subsiding regions, hereinafter called "dry holes"<sup>2</sup> for the sake of brevity, was noted in GATE by Gray and Wylie (1975) who observed these regions to be from 10 to 50 km wide and more or less sharply bounded. The region discussed here is probably of the same kind, being about 12 km across and sharply bounded as will be shown hereafter. The author is unaware of any published data describing the small-scale structure of a dry hole and certainly there are none reported for the scales considered here. Profiles of air temperature and relative humidity for 1502-1507 GMT are shown in Fig. 1. The figure is also used to delineate separate phases of the penetration for analysis. Phase I (from before 1500 to 1503:20) represents the normal external environment as does Phase V (from 1505:44 on). These are called pre-entry and post-exit phases, respectively. Phase II (1503:25 to 1503:54) is a sharp transition region called the entry phase. It is probably a region of high shear and is certainly not inertial. Phase III is somewhat like Phase II. It is called the exit ramp. Phase IV (1504:37 to 1505:24) is a region of little change which appears to be well within the hole on the exit leg of the penetration. It is called the exit plateau. Fig. 2 shows a time series of the horizontal velocity fluctuations  $U'$  along the flight path for the period covered by Fig. 1. The trace is noticeably different in the three middle phases. It was this peculiar time trace that first suggested the presence of unusual characteristics in the region and led to detailed investigation of the aircraft records. The small-scale structure of the region was quite unexpected.

### 3. Time series of turbulence intensity along the flight path

While time series of the raw variables may be useful for diagnostic purposes as in Fig. 2 above, the frequency response of the system was not designed to cover the

<sup>2</sup> The term was coined, as far as the author is aware, by Dr. Bradford Bean of NOAA's Boundary Layer Dynamics Group, who described a similar event in a private communication to the author.

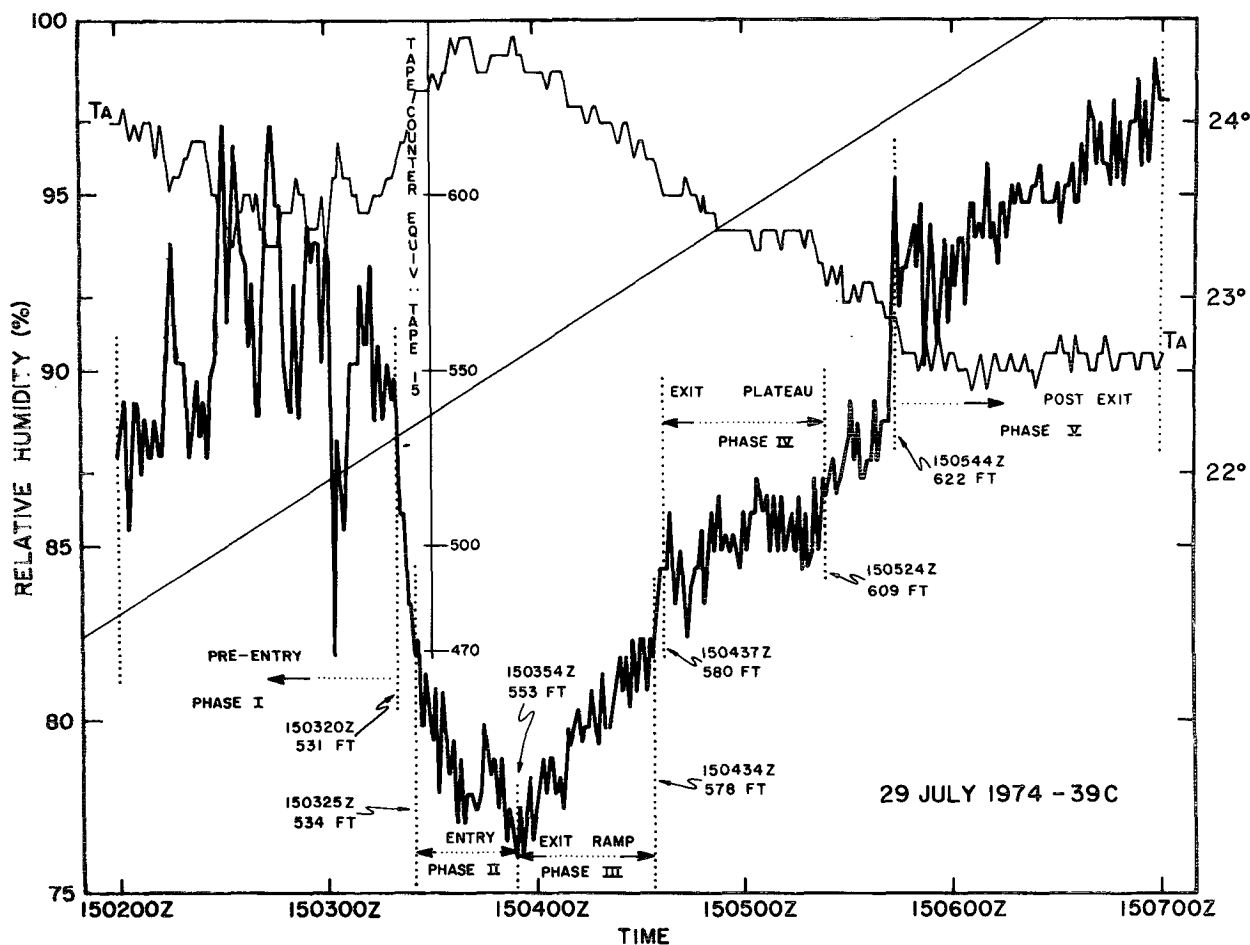


FIG. 1. Temperature and relative humidity across a dry hole with phases identified.

energy-containing range of turbulence for which  $U'$  is an appropriate measure. Because we have limited our observations to the finestructure, a better measure of the turbulence intensity is the dissipation rate. When intercomparing velocity components and temperature, the appropriate measure is the power spectral density at a common frequency. Time series of these quantities will be used to represent the turbulence intensity along the flight track.

Fig. 3 presents  $\epsilon$  as a function of time for the entire observation period. The intermittent character of the turbulence is obvious. Local variations of  $\epsilon$  approaching two orders of magnitude may occur in a distance of less than 1 km (e.g., near 1452:30), while general trends with an amplitude of an order of magnitude or more occur on scales of tens of kilometers (e.g., 1535–1545). The variation in  $\ln \epsilon$  seems to be as large at 900 m (tape 17) as at 150 m (Tapes 14, 15, 16) even though the mean level at 900 m is an order of magnitude smaller.

Fig. 4 allows comparison of the time variations of the 472 Hz spectral density of  $U'$ ,  $W'$  and  $T'$  across

the dry hole where the environment changes radically as do the spectral shapes of  $U'$ ,  $W'$  and  $T'$  which will be described later. While the intensities of the several variables usually seem to vary in a similar manner (e.g., examine the region from 1450 to 1456), in the dry hole (1503–1506) the  $W'$  component is selectively suppressed with only a slight change in  $U'$  and none in  $T'$ . The apparent inequality generally of the  $U'$  and  $W'$  spectra should not be taken seriously because of the large total error (6 dB) possible in scaling  $W'$  relative to  $U'$  as described by Merceret (1976), but the relative variations are real. The selective suppression of  $W'$  in the dry hole is probably due to buoyancy, though it is surprising to see an anisotropic buoyancy effect at scales so small.

#### 4. The probability distribution of $\ln \epsilon$

It appears that near log-normality of the dissipation distribution as suggested by Kolmogorov (1962) may be a more universal property of atmospheric turbulence than local isotropy of inertial behavior at small scales.

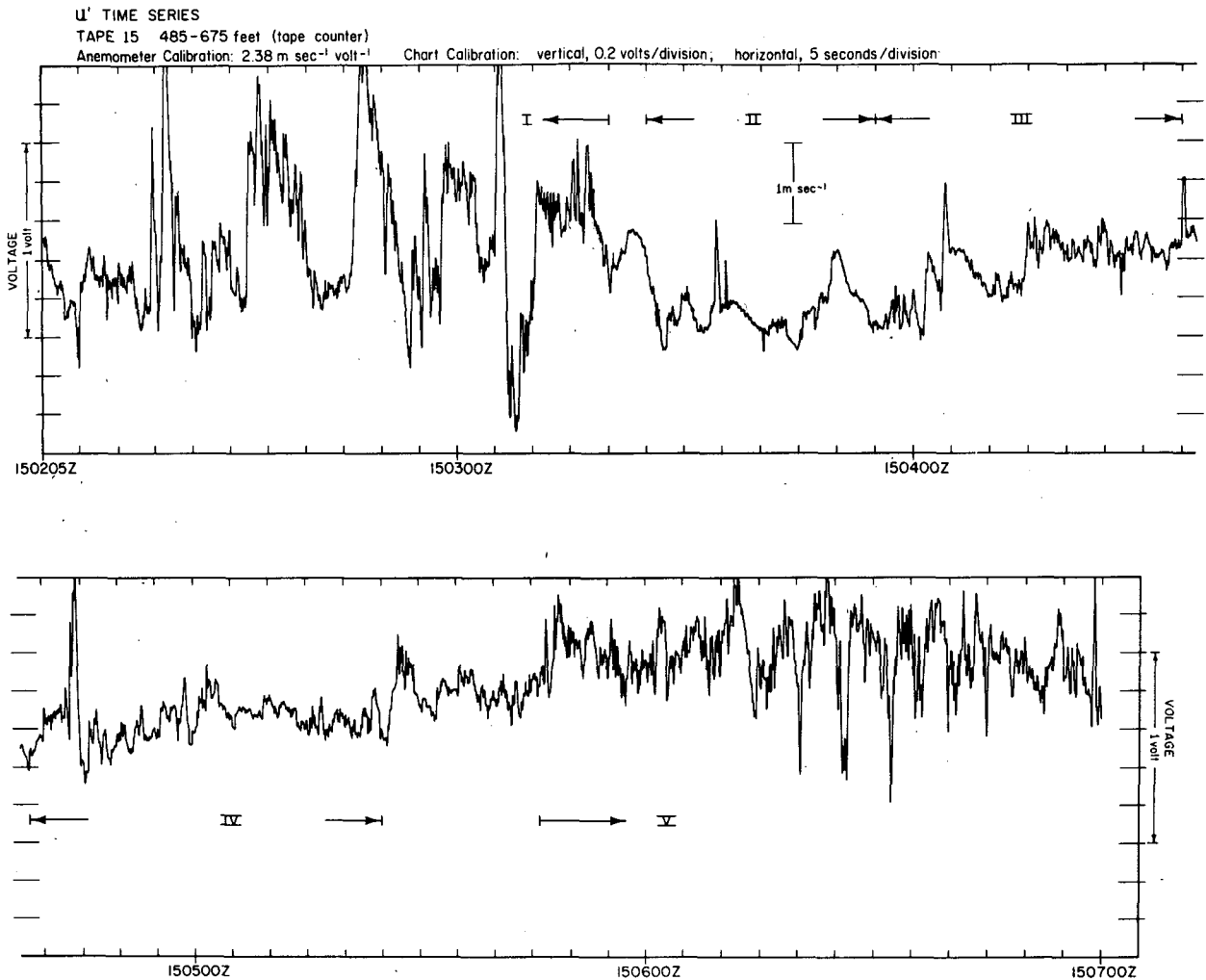


FIG. 2. Time series of horizontal velocity fluctuations across a dry hole.

Fig. 5 shows probability distributions computed in both normal regions (Phases I and V) and dry hole regions of the atmosphere. In the dry hole it is not clear that (2a) may be used to compute  $\epsilon$  since the spectra do not obey (1), but the  $W'$  spectrum is the least deviant and is close to (1). Recognizing that the conversion from power spectral density to  $\epsilon$  using (2a) may not be rigorously warranted, it does seem likely that it remains a reasonable approximation. To the extent the approximation is valid, it is remarkable how little the distribution differs between the normal and dry regions. (The comparison is made only after allowing the arbitrary dissipation scale to be shifted so that the 50% probability points overlap. Thus we take into account the different turbulence levels.) The distribution is log-normal over most of its range. The "droop" at the low probability end may be influenced by the low signal-to-noise ratio there because low probability is associated with lowest signal levels in the system, but the signal-to-noise problem is probably

not sufficient to account for the entire departure from log-normality below the 20% level. On the other hand, clipping caused by peaks exceeding the dynamic range of the probability analyzer almost certainly accounts for the deviation from log-normality at the 99% level.

Better instrumentation and more sophisticated data processing techniques should make studies of the probability distribution of  $\ln \epsilon$  in various environments of the atmosphere a fruitful area for continued investigation.

### 5. Spectra of $U'$ , $W'$ and $T'$

Figs. 6, 7, and 8 present  $U'$ ,  $T'$  and  $W'$  spectra respectively for various phases of the dry hole penetration. Each phase is identified and a quick intercomparison can be made. The spectra presented for each phase begin where indicated in the figure and continue over the entire phase for Phases II, III and IV, while those for Phases I and V are 64 s averages. A line of

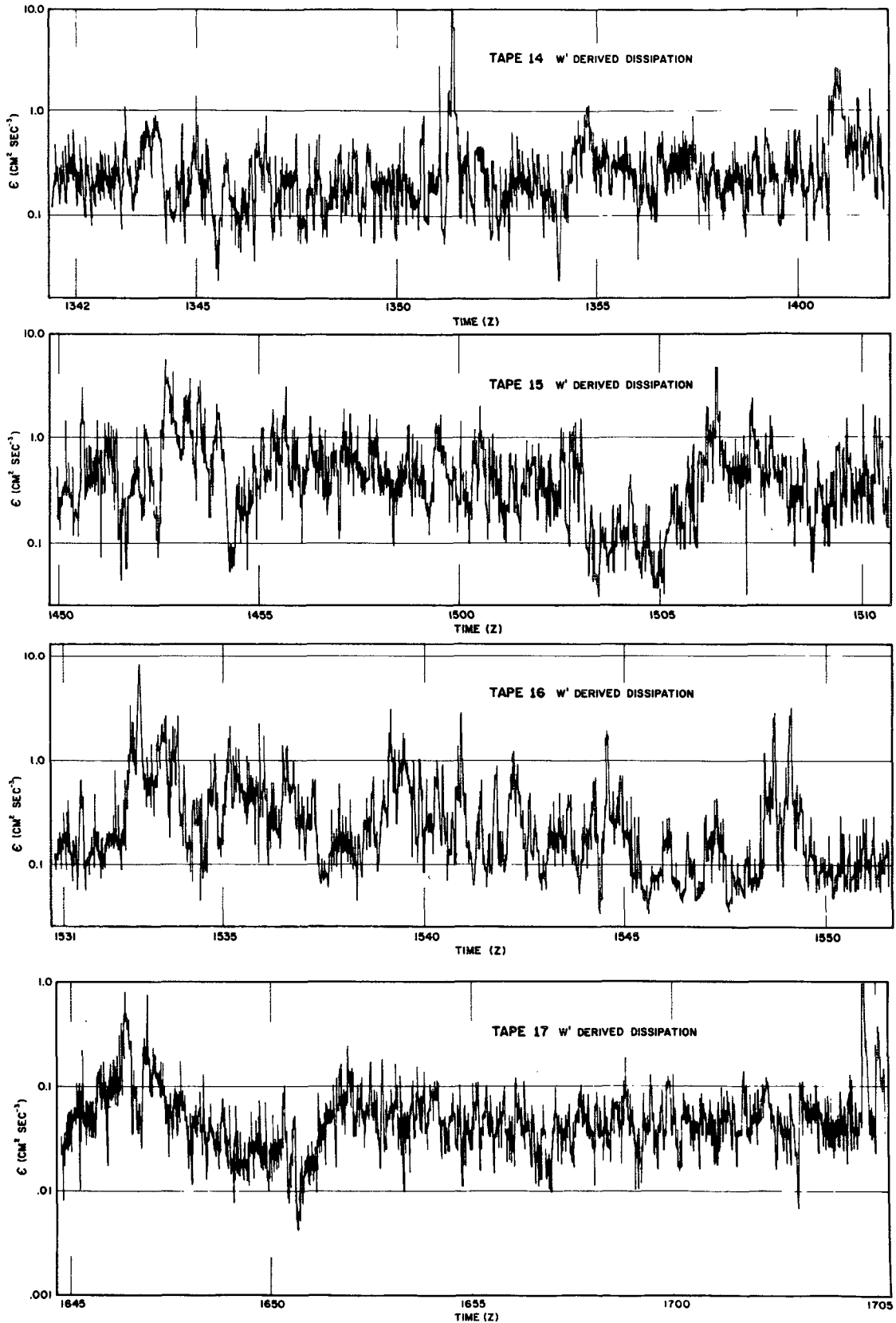


FIG. 3. Time series of  $\ln \epsilon$  for the observation period.

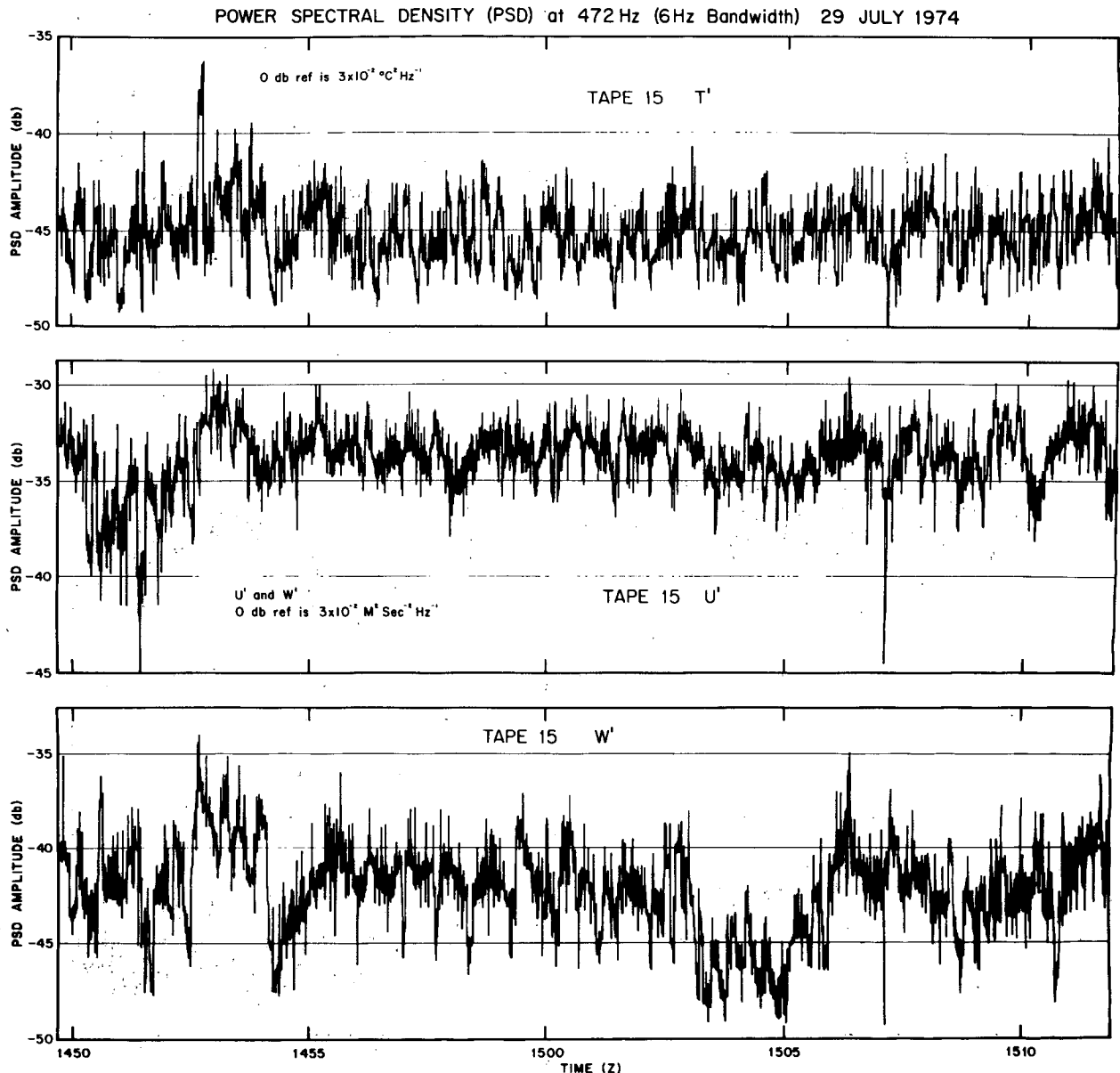


FIG. 4. Time series of power spectral density of  $U'$ ,  $W'$  and  $T'$  at 472 Hz across a dry hole.

slope  $-5/3$  is included for reference only and is not fitted to any of the data. Phase II behaves strangely in each of the three variables. Its slope is much less than the  $-5/3$  we would expect to find in an inertial subrange until a frequency of about 100 Hz (equivalent to a scale of about 1 m) is reached. This behavior is less pronounced in the  $W'$  spectrum than in the other two. Even above 100 Hz the ratio  $U'_{II}/U'_I (\approx 1)$  does not equal the ratio  $W'_{II}/W'_I (\approx 0.1)$ . Thus, if the turbulence of Phase I is nearly isotropic, the turbulence of Phase II cannot be isotropic, even at scales  $< 40$  cm.

Phases III and IV also exhibit a strong deviation of  $W'$  from the behavior of  $U'$  and  $T'$  at the higher frequencies. In all phases  $U'$  and  $T'$  approach common

values above 100 Hz, but  $W'$  in the dry region remains an order of magnitude lower than in the outside environment. If the dry region is, indeed, descending and stable, then this quality is consistent with selective buoyant suppression of the vertical velocity at a rate faster than can be compensated for by the tendency to isotropy. Measurements to scales as small as 5 cm (2 kHz) showed no indication of the existence of a classical inertial subrange in this situation.

The spectrum of Phase IV is typical of anomalous regions occupying 10–15% of the records we obtained. The spectrum of Phase II is not typical of anything found frequently. Phases I and V are typical of about 80% of our records. While it matters a great deal what

kind of region one examines, within a given region of any type it does not matter whether there is precipitation. This may not be true for heavier rainfall rates such as those of tropical storms. The heaviest rainfall encountered in this experiment was  $\sim 25 \text{ mm h}^{-1}$ .

In addition to the effects of a varying environment, the spectra also show the effect of high Reynolds number intermittency on the slope of the temperature spectrum implied by its effect on the structure function as computed by Tennekes (1973). As Busch *et al.* (1973) have suggested, these effects are too small to be seen in the velocity spectra alone with accuracies as limited as those obtainable here. The relative effect on the temperature spectrum shows nicely, however. These effects are predicted on the basis that  $\epsilon$  has a log-normal probability distribution. This is consistent with the probability distribution we measured.

Because of the marginal signal-to-noise ratio obtained at 900 m, only the  $W'$  spectrum is presented for this altitude (Fig. 8). Its level is significantly lower than that obtained under normal conditions at 150 m as one would expect. Its shape and slope are consistent with the existence of an inertial subrange. More sophisticated analysis of the data from 900 m would require better signal levels than we obtained.

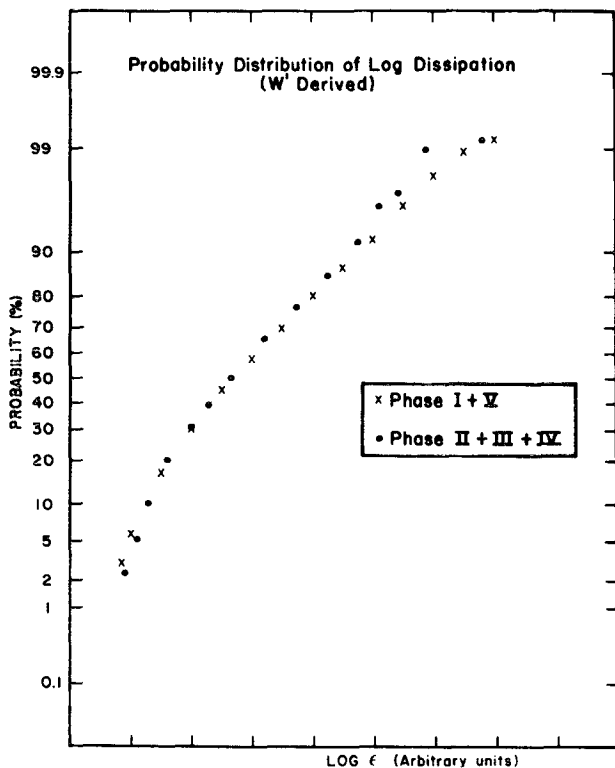


FIG. 5. Probability distributions of  $\ln \epsilon$  for various phases of dry hole penetration.

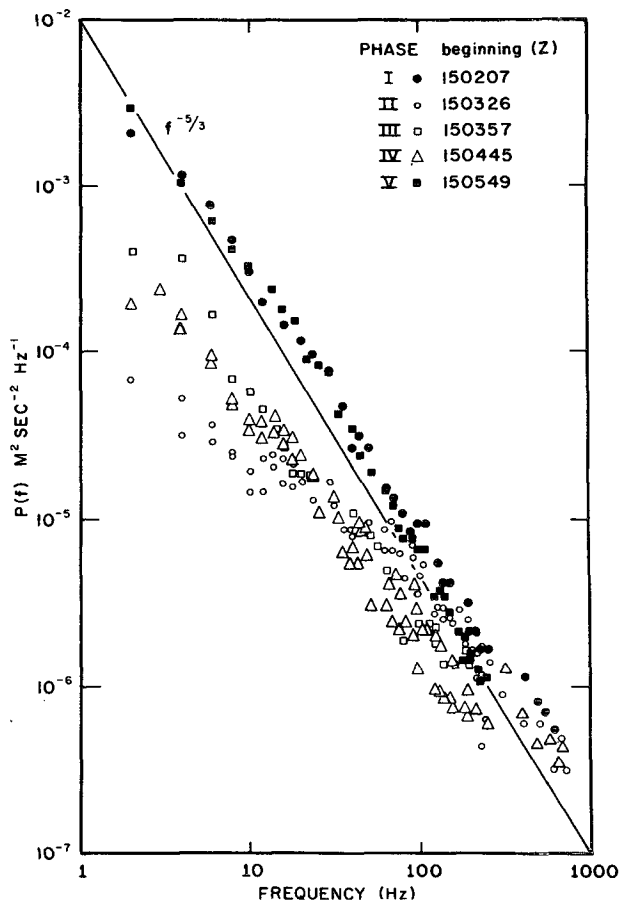


FIG. 6.  $U'$  spectra for various phases of dry hole penetration.

### 6. Conclusions

There are two major and complementary conclusions to be drawn from these results. The first is that the microstructure must be measured if dissipation is to be accurately computed for meteorological purposes, because the simplifications of local isotropy and inertial subrange behavior are not universally valid until scales of a few meters or less are reached. This is highlighted by the microstructure of the dry hole. It is not isotropic (not even locally), and it does not possess inertial subrange properties. The dry hole does, however, share log-normality of its dissipation distribution with its more normal surroundings, to the extent that one can hope to infer dissipation from non-inertial spectra.

The existence of sizable regions of peculiar or atypical behavior has the potential for hindering boundary layer studies, most of which rely on a substantial degree of horizontal homogeneity for averaging purposes and analytic descriptions. Conditional sampling techniques may aid such studies. In any case, more work at all scales in the vicinity of atypical regions like the one described here is required. In the

long run, we may have to redefine or even abandon the term "typical" in our discussions of the tropical boundary layer.

The second conclusion is that the atmosphere makes a fine laboratory for the study of high Reynolds number intermittent turbulence for its own sake. The result here tending to support Kolmogorov's (1962) log-normal prediction, at least over the middle of the probability range, is just one example of the kind of basic turbulence research that may be conducted in the atmosphere, but with great difficulty, if at all, in the laboratory where high Reynolds numbers are hard to achieve at low Mach numbers. Continued investigation of the structure of the atmosphere at scales from 100 m to about 1 cm will benefit meteorologists and turbulence investigators alike.

*Acknowledgments.* The United States GATE Project Office funded this research throughout. Their continued support has been essential and is deeply appreciated. Thanks to Jim McRory of the Research Facilities Center, and John Cuning of the National Hurricane and Experimental Laboratory (NHEML) for help with the instrumentation and observations. Brian Rice of NHEML reduced much of the data.

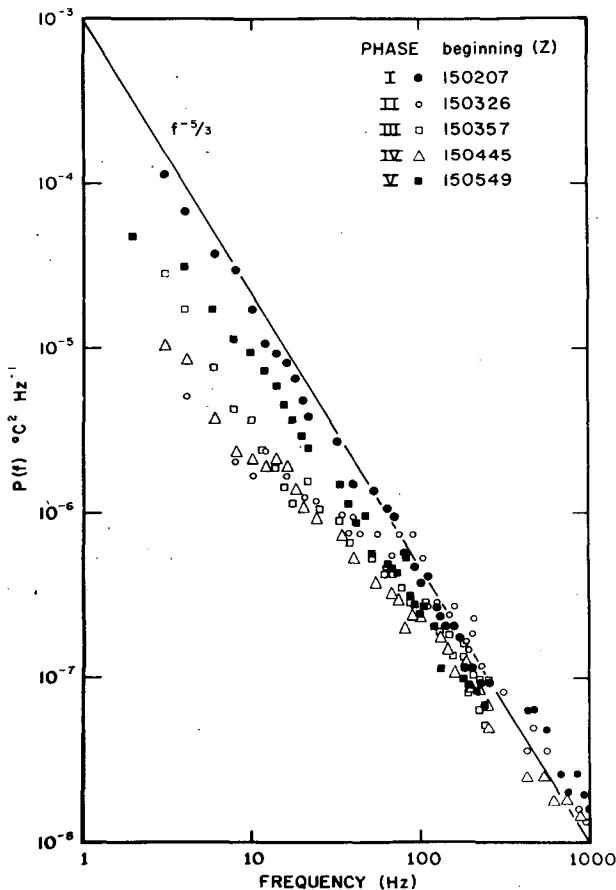


FIG. 7.  $T'$  spectra for various phases of dry hole penetration.

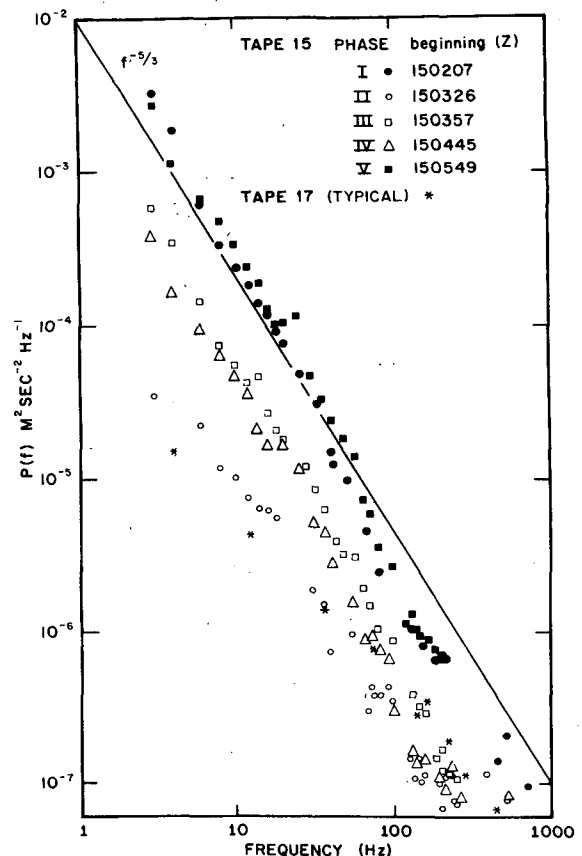


FIG. 8.  $W'$  spectra for various phases of dry hole penetration and for the leg at 900 m altitude.

Dale Martin and Charles True of NHEML produced the figures for this paper. The author appreciates the contributions of a reviewer which led to a substantial improvement of the paper.

REFERENCES

Bendat, J. S., and A. G. Piersol, 1966: *Measurement and Analysis of Random Data*. Wiley, 390 pp.  
 Boston, Noel E. J., and R. W. Burling 1972: An investigation of high-wavenumber temperature and velocity spectra in air. *J. Fluid Mech.*, **55**, 473-492.  
 Busch, Niels, E., B. R. Bean, Y. Furuhashi, G. A. McBean and J. Strohben, 1973: Turbulence spectra at scales smaller than 1 meter. *Bound.-Layer Meteor.*, **5**, 211-217.  
 Gray, William M., and Donald Wylie, 1975: Preliminary analysis of a selective sample of GATE ship and aircraft data. Preliminary scientific results (Vol. II), GATE Report 14, GARP, ISMG, WMO, 188-190.  
 Kolmogorov, A. N., 1962: A refinement of previous hypothesis concerning the local structure of turbulence in a viscous incompressible fluid at high Reynold's number. *J. Fluid Mech.*, **13**, 82-85.  
 Lumley, J. L., and H. A. Panofsky, 1964: *The Structure of Atmospheric Turbulence*. Wiley, 239 pp.  
 Merceret, Francis J., 1976: Measuring atmospheric turbulence with airborne hot-film anemometers. *J. Appl. Meteor.*, **15**, 482-490.  
 Tennekes, H., 1973: Intermittency of the small-scale structure of atmospheric turbulence. *Bound.-Layer Meteor.*, **4**, 241-250.